

**THE EFFECT OF UPSTREAM FLOW CONDITIONS TO LAMINAR MIXING IN A MINIATURE COMBUSTION CHAMBER**

Peter L. Woodfield / Kyoto University

Kazuya Tatsumi / Kyoto University

Kazuyoshi Nakabe / Osaka Prefecture University

Kenjiro Suzuki / Kyoto University

**ABSTRACT**

A three-dimensional unstructured finite-volume method is used to investigate laminar flow characteristics of a miniature chamber with a possible application to micro gas turbine combustor design. The chamber is cylindrical in shape and 20mm in diameter with the fuel stream entering via a single jet in the center of one end of the can. Oxidizer jets are generated by a circular baffle plate having six holes surrounding the fuel jet. Attention is given to the effect of the inlet conditions on the flow structure and mixing pattern inside the chamber. Computations are carried out with the calculation domain inlet being positioned at two different locations; (1) at the immediate entrance to the combustion chamber (2) one combustor diameter upstream of the baffle plate. Numerous inlet conditions are considered including 'top-hat', fully-developed, swirling, an annular backward facing step and some asymmetrically skewed profiles. The baffle plate is shown to have a significant smoothing effect on the inlet conditions for a Reynolds number of 100.

Previously, the authors considered the effects of the size and positioning of the jets in the present design for laminar conditions [2]. The goal of the present study is to continue the study on the laminar flow case and in particular to focus on the effects of the inlet conditions upstream of the baffle plate to the mixing patterns in the chamber. To separate the effects of chemical reaction and fluid dynamics, the results presented are for isothermal constant density flow.

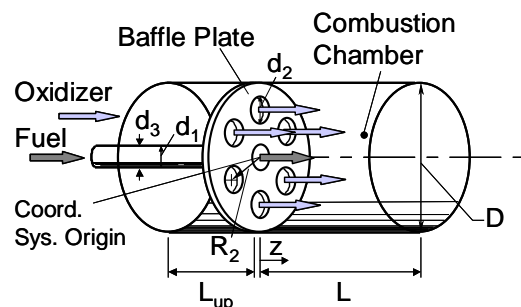


Fig. 1 Geometry for investigation.

**INTRODUCTION**

The present study is part of an ongoing project to develop a miniature can-combustor for a micro gas turbine (MGT; 5 - 100 kW) to be used in a hybrid MGT – solid oxide fuel cell (SOFC) distributed energy system [1]. The device could ultimately be used for electricity production in individual houses or for small communities. Hence it is essential that each component in the system is compact, safe and reliable. To meet the first of these requirements, the physical size of the combustion chamber is expected to be restricted to the order of 20mm in diameter and 200 mm in length. Thus simulation of gas mixing in small chambers is considered an important topic for investigation within the overall framework of the project. The device itself could be designed to operate under either laminar or turbulent flow conditions.

Figure 1 shows the geometry under consideration. The fuel enters the chamber as a single jet in the center of one end and the oxidizer jets are produced by a circular baffle plate having six holes surrounding the fuel jet.

**NOMENCLATURE**

$b_{th}$	thickness of baffle plate
$d_1$	inside diameter of fuel tube
$d_2$	diameter of oxidizer holes
$d_3$	outside diameter of fuel tube
$D$	diameter of can
$L$	length of domain downstream of baffle plate
$L_{up}$	length of domain upstream of baffle plate
$L_1$	distance upstream of baffle plate to back-step
$p$	pressure
$R_1$	radius for top of annular step
$R_2$	radial position of center of oxidizer holes
$Re_D$	Reynolds number, $\rho U D / \mu$
$U$	mean velocity over can cross-section
$u_i$	'i'th component of velocity

$x_i$	Cartesian coordinate
$x$	Cartesian coordinate ( $= x_1$ )
$y$	Cartesian coordinate ( $= x_2$ )
$z$	Cartesian coordinate ( $= x_3$ )

#### Greek symbols

$\mu$	dynamic viscosity
$\xi$	mixture fraction
$\rho$	density
$\sigma$	Schmidt number
$\phi$	dependent variable

### GOVERNING EQUATIONS

Three-dimensional incompressible continuity (Eq. (1)) and Navier-Stokes equations (Eq. (2)) are solved for steady state conditions.

$$\frac{\partial u_j}{\partial x_j} = 0 \quad (1)$$

$$\frac{\partial}{\partial x_j} (\rho u_j u_i) = -\frac{\partial p}{\partial x_i} + \frac{\partial}{\partial x_j} \left( \mu \frac{\partial u_i}{\partial x_j} \right) \quad (2)$$

The calculation is treated as a constant property, two-stream mixing problem and Eq. (3) is solved for the mixture fraction,  $\xi$ , (mass fraction of gas which originated in the fuel stream) under non-reacting (cold flow) conditions.

$$\frac{\partial}{\partial x_j} (\rho u_j \xi) = \frac{\partial}{\partial x_j} \left[ \frac{\mu}{\sigma} \frac{\partial \xi}{\partial x_j} \right] \quad (3)$$

### NUMERICAL METHOD

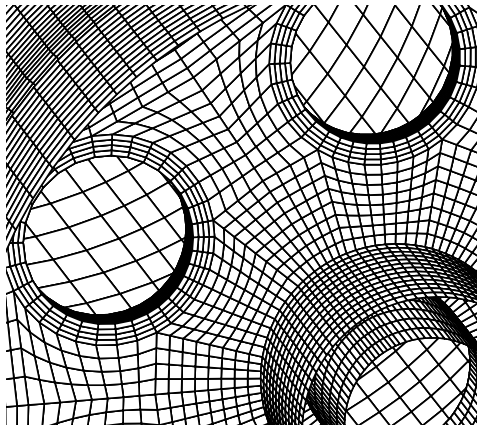


Fig. 2 Computational mesh on surface of domain viewed from the upstream side of the baffle plate.

A three-dimensional unstructured finite-volume procedure [3] is used to discretize the governing equations, Eq. (1) ~ (3). A second-order upwind biased scheme is used for the convection terms and the Rhie/Chow approach [4] is used to prevent checker-board oscillations in the pressure field. The SIMPLE algorithm is employed to couple velocity and pressure via the continuity equation. Median-dual control volumes based on a hexahedral mesh are used for numerical integration. Fig. 2 gives a close-up three-dimensional view of part of the

computational grid on the surface of the domain. The view is from the upstream side of the baffle plate. Using finer grid spacing produced little change to the results indicating that the chosen spacing was fine enough for the present study.

### CODE VALIDATION

The computer code used for this study was written by the first author and has been tested and found to perform well [3] for a range of laminar flows including pipe flow, flow in an eccentric annulus, backward facing step flow and flow for a compact fin and tube heat exchanger element. Low sensitivity to grid arrangement and orientation also has been demonstrated for practical grid spacing [3] at Reynolds numbers similar to those used in the present study. Figure 3 shows the centerline velocity distribution for a three-dimensional lid-driven cavity flow against the benchmark finite-element results of Jiang et al. [5]. The grid allocation was similar to that used in the benchmark test. The good agreement shown is a further example of the validity of the present numerical procedure.

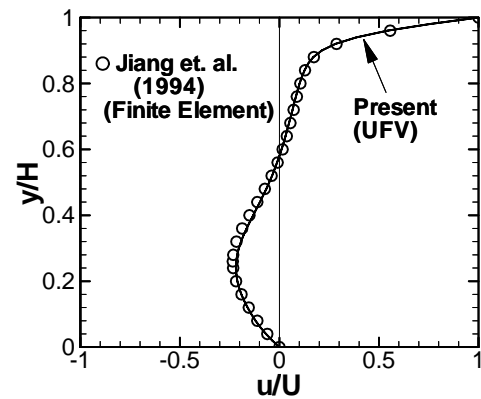


Fig. 3 Centerline velocity distribution for a lid-driven cubic cavity flow.

### DOMAIN AND BOUNDARY CONDITIONS

Figure 1 shows the domain of the computation for the present study. Table 1 gives the specific details of the geometry used in this study. All solid surfaces are treated with the no-slip condition for velocity and the zero-flux condition for the species conservation equation. The outlet which is located at  $L = 15$  diameters downstream of the baffle plate utilizes a zero normal gradient boundary condition for components of velocity and the mixture fraction. The location of the inlet and the choice of inlet velocity profiles were varied as the theme of this present study and thus are not given in Table 1. In all cases however, the ratio of fuel to oxidizer mass flow rate was kept constant at  $m_1/m_2 = 0.0488$  which corresponds approximately to a methane/air combustor operating with 18% excess air. Unless otherwise stated, the Reynolds number,  $Re_D$ , was set at 100 based on the diameter of the can,  $D$ , and the bulk velocity,  $U$ , on the downstream side of the baffle plate. For these flow conditions, the authors previously found that the specifications in Table 1 give close to the optimum mixing rate for the present design [2].

Table 1 Geometry for computation domain.

$d_1/D$	$d_2/D$	$R_2/D$	$b_{th}/D$	$d_3/D$	$L/D$
0.182	0.182	0.341	0.05	0.282	15

### OVERALL PERFORMANCE OF DESIGN

Previously, the authors considered the performance of the present design for a range of hole locations and sizes [2]. In comparison to the confined co-axial jet with the same flow rates of fuel and oxidizer, the present arrangement was found to perform extremely well. Figure 4 reiterates this finding where it is clear that the baffle plate contributes significantly to the mixing compared with the case where no baffle plate is present.

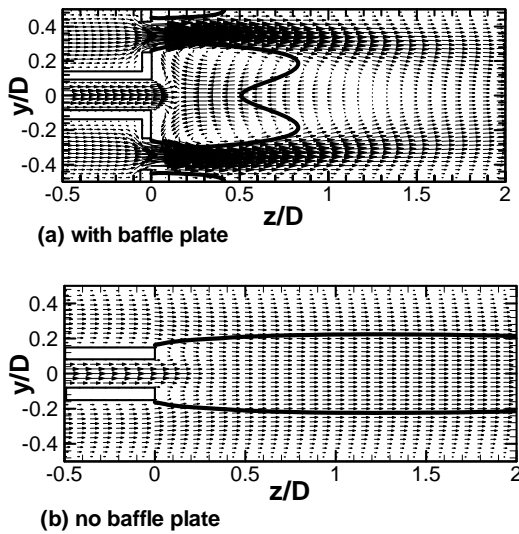


Fig. 4 Overall effect of baffle plate - velocity vectors ( $x = 0$  plane). The solid line represents the mixture fraction iso-surface,  $\xi = 0.055$ .

### SENSITIVITY TO OUTLET LOCATION

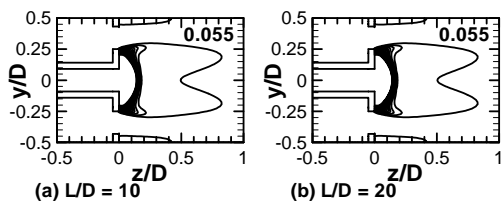


Fig. 5 Mixture fraction contours. Effect of choice of domain outlet location ( $x = 0$  plane).

Before considering the sensitivity to the inlet velocity profiles, it is useful to confirm that the computational domain has been made long enough so that the outlet position has little influence on the results. For the present study, the outlet was positioned at 15 diameters downstream of the baffle plate. Figure 5 shows mixture fraction contours in the  $x = 0$  plane for

the outlet positioned both at 10 and 20 can diameters downstream of the baffle plate. Since the results shown for the two cases are almost identical it is considered that the length of 15 diameters is more than adequate for the present study.

### EFFECT OF CALCULATION INLET LOCATION AND VELOCITY PROFILE

To test the importance of the choice of inlet location, calculations are performed with the computational domain beginning at the entrance to the combustion chamber (Figs. 6 (a) and (b)) and with the inlet specified one diameter upstream of the baffle plate (Figs. 6 (c) and (d)). For both cases two different inlet velocity profiles are considered – the Poiseuille profile (Figs. 6 (b) and (d)) and the top-hat profile (Figs. 6 (a) and (c)).

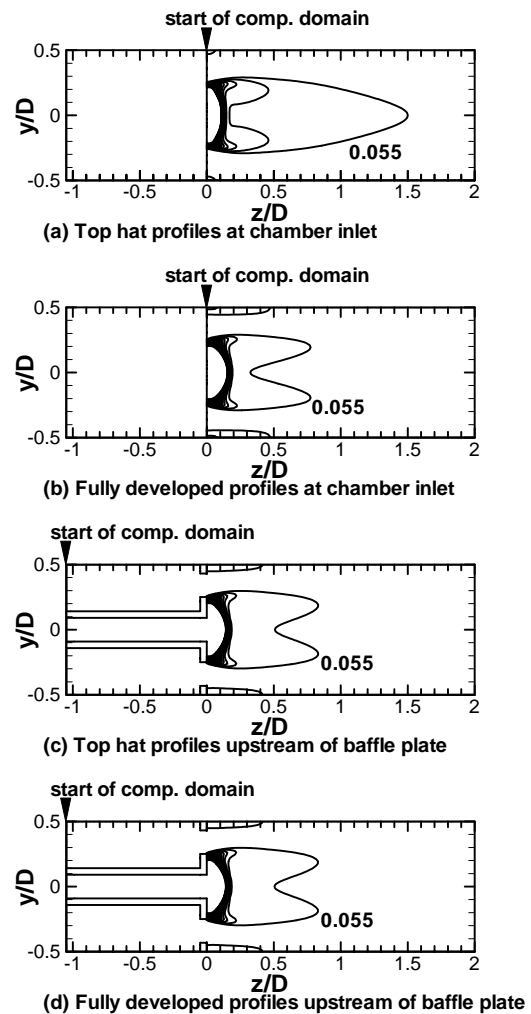


Fig. 6 Mixture fraction contours showing effect of choice of inlet location for computational domain ( $Re_D = 100$  and  $x = 0$  plane).

As can be seen in Fig. 6, the results are reasonably sensitive to the inlet velocity profile if it is specified at the inlet to the combustion chamber (Figs. 6 (a) and (b)). However, if

the upstream region is included (Figs. 6 (c) and (d)) changing the velocity profile from a top-hat profile to the Poiseuille profile has a negligible effect on the predicted mixture fraction contours inside the chamber. Hence it is better to commence the calculation upstream of the baffle plate and we may expect that at one diameter upstream of the inlet a partially developed or fully developed symmetrical profile will not have a major effect on the mixing pattern inside the chamber for  $Re_D = 100$ .

### EFFECT OF INLET SWIRL

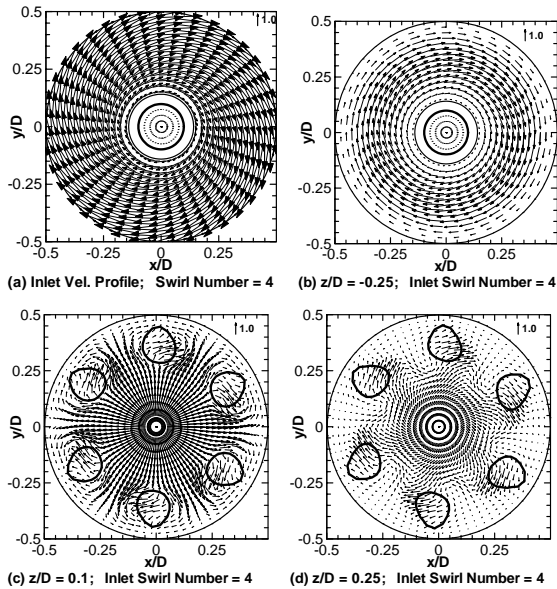


Fig. 7 Velocity vectors for swirl number = 4. The solid line is the mixture fraction contour for  $\xi = 0.055$ .

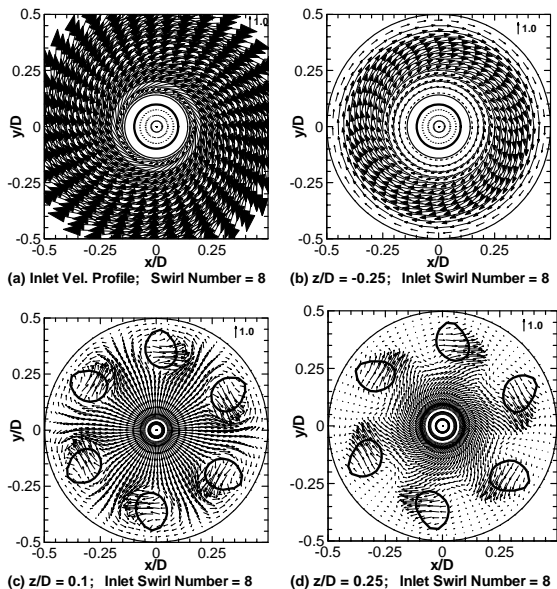


Fig. 8 Velocity vectors for swirl number = 8. The solid line is the mixture fraction contour for  $\xi = 0.055$ .

Many practical combustors aim to make use of a swirling flow field to enhance the mixing performance and achieve stable combustion. Thus it is useful to consider the effect of a swirling inlet profile within the framework of the present study. However, from the results shown above in Fig. 6 we might expect that introducing swirl on the upstream side of the inlet may not be so effective. This is confirmed in Figs. 7 and 8. Figures 7 and 8 show velocity vectors at a number of axial positions for swirling profiles introduced one diameter upstream of the baffle plate. The length of the vector arrows are scaled against the same reference vector so it is possible to see how the swirl component diminishes with downstream distance by comparing Figs. 7 (a), (b), (c) and (d).

Figure 7 shows results for an inlet swirl number of 4 where the swirl number is defined as the maximum inlet tangential component of velocity divided by the mean axial component of velocity. Figure 8 shows the same  $z$  – cross sections for a swirl number of 8.

We can see from Figs. 7 and 8 that the baffle plate very effectively damps out even a large component of swirl if introduced one diameter upstream of the plate. The small component of swirl that finally enters the combustion chamber itself appears to contribute only a little towards enhancing the mixing as is shown in Fig. 9.

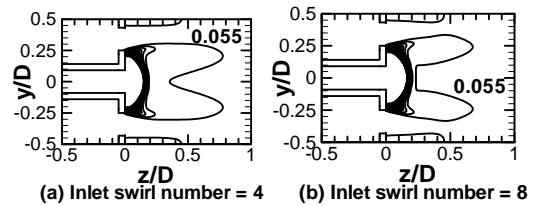


Fig. 9 Mixture fraction contours ( $x = 0$  plane).

Thus, the results of this section suggest that introducing swirl on the upstream side of the baffle plate may not be the best approach to create a strongly swirling flow field in the combustor. Also, noting the observations made concerning Fig. 6, perhaps a more effective approach to introduce swirl would be to change the angles of the jets as they enter the combustion chamber by boring the holes in the baffle plate itself at angles offset from the perpendicular.

### EFFECT OF INLET ASYMMETRY

While the baffle plate may have a tendency to damp out some desirable inlet features such as swirl introduced on the upstream side of the plate, we can also expect that it will reduce the effects of undesirable inlet features such as asymmetry in the inlet profile. This is an important consideration since the size constraints on the practical design may make it difficult to completely smooth out the inlet velocity profile.

Figure 10 (a) shows the effect of specifying an inlet velocity distribution which is tilted slightly about the  $x$ -axis so that the velocity is 5% higher than the mean at  $y/D = 0.5$  and 5% lower at  $y/D = -0.5$ . Figure 10 (b) shows the corresponding case for a 20 percent departure from a uniform inlet velocity profile.

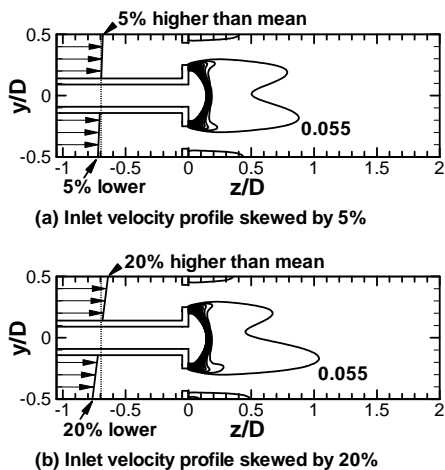


Fig. 10 Mixture fraction contours showing effect of asymmetry in the inlet velocity profile ( $x = 0$  plane).

From Fig. 10 (a) it is apparent that for the case of a Reynolds number of 100, a five percent departure from a symmetrical profile at one diameter upstream of baffle plate produces only a very small effect on the symmetry of the mixing pattern inside the combustion chamber. Figure 10 (b) indicates that an increase to 40 percent variation across the inlet profile does have a noticeable effect on the mixture fraction field. Thus, we can conclude that it is desirable to keep the flow pattern upstream of the baffle plate symmetrical but with the present geometry and flow conditions, a small departure from symmetry at one diameter upstream of the inlet may be forgivable.

### EFFECT OF PROXIMITY TO BAFFLE PLATE OF UPSTREAM CHANGES IN GEOMETRY

In the above sections the effectiveness of the present design in smoothing out a number of different profiles specified at one diameter upstream of the baffle plate was demonstrated. We will now examine how close to the baffle plate it is possible to introduce a change in geometry before having a major effect on the flow field inside the chamber. This is an important consideration for the present application which, as mentioned above, is likely to have restrictions placed on the maximum size of the inlet passage. For this test we have selected to introduce an annular backward facing step upstream of the baffle plate.

The top of the step is specified by  $R_1$  in Fig. 11 (a) which for the present study is set equal to  $R_2$  (cf. Fig. 1 and Table 1). Figure 11 shows the effect of varying the upstream location of the step denoted  $L_1$  as shown in Fig. 11 (a).

The similarity between Figs. 11 (a) ~ (c) and 5 (c) makes it clear that for  $Re_D = 100$  the step has little influence on the mixing pattern so long as it is positioned greater than about  $0.5D$  upstream from the plate. On the other hand, if very close to the plate as in Figs. 11 (d) and (e) the position of the step has a significant effect on the mixing pattern. In both Figs. 11 (d) and (e) the mixing is evidently slower than in Figs. 11 (a) and (b). However, the fuel-rich region near the wall in Fig. 11 (a) has been reduced in size in Figs. 11 (d) and (e). This may be

desirable for a practical combustor. Hence from another aspect, introducing a movable backward facing step on the upstream side of the baffle plate could result in an adjustable device capable of fine-tuning the mixing pattern.

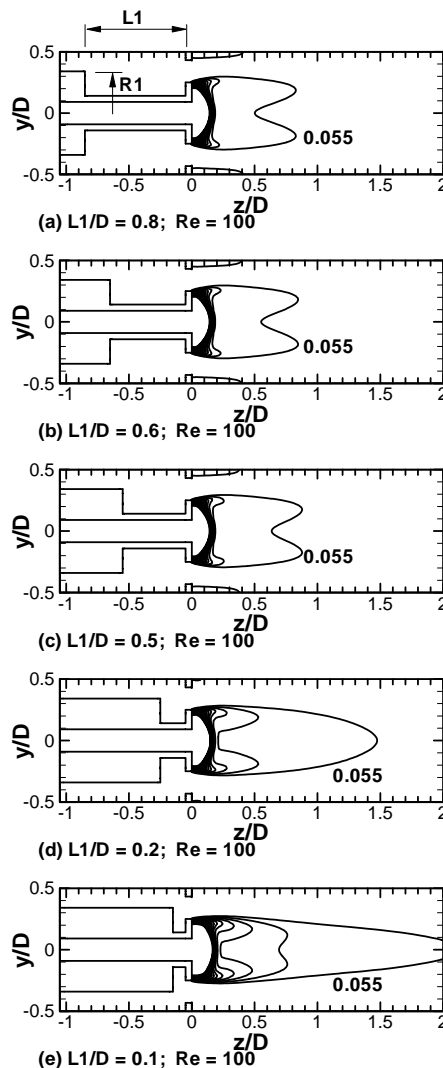


Fig. 11 Mixture fraction contours – effect of adding an annular backward facing step upstream of the baffle plate ( $Re = 100$  and  $x = 0$  plane).

### EFFECT OF INCREASING REYNOLDS NUMBER

All the cases considered in the previous sections have been for a Reynolds number of 100 based on the mean flow and can diameter. At higher Reynolds numbers we may expect that the upstream inlet conditions will become more important for laminar flow. To examine this effect, in Fig. 12 we have repeated the cases shown in Fig. 11 but with  $Re_D = 200$ . For all cases again we have maintained the same fuel/oxidizer ratio and all inlet conditions are symmetrical.

It is apparent from Fig. 12 (a) that the mixing performance of the present design is still very good at the higher Reynolds number. Comparing Figs. 11 (a) and 12 (a) it is clear from the location of the iso-surface for  $\xi = 0.055$  that the mixing field

generally expands in the downstream direction for an increase of Reynolds number. However, unlike laminar coaxial jet flow (cf. Ref. [2] for example), the expansion is not in direct proportion to  $Re$  for every feature of the flow.

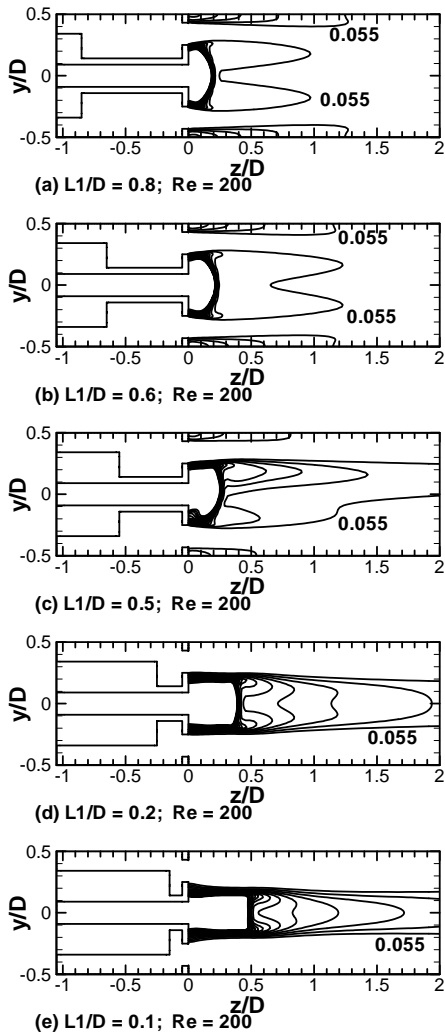


Fig. 12 Mixture fraction contours – effect of adding annular backward facing step upstream of baffle plate ( $Re_D = 200$  and  $x = 0$  plane).

Another important observation from Fig. 12 is that at higher Reynolds numbers, the position where the inlet conditions start to become important is further upstream than at lower  $Re_D$ . It should be noted here that the results for Fig. 12 (a) are almost identical to the  $Re_D = 200$  case without the step (not shown). Comparing Fig. 12 (a) with Fig. 12 (b), the positioning the step at 0.6 diameters upstream of the baffle plate in the case of  $Re_D = 200$  has a noticeable influence on the mixing pattern in the chamber where almost no change is observed for the same position with  $Re_D = 100$  (cf. Figs. 11 (a) and (b)).

It also should be noted that there is a dramatic difference in the mixing pattern for Figs. 12 (b), (c) and (d). This in part can be explained through an examination of the respective flow fields. Before examining the non-symmetrical case Fig. 12 (c),

for clarity of the discussion it is easier to compare cases Fig.s 12 (b) and (d). Figure 13 shows the flow patterns in a z-cross section located at  $z/D = 0.1$  for the step positioned at  $L1/D = 0.6$  and at  $L1/D = 0.2$ .

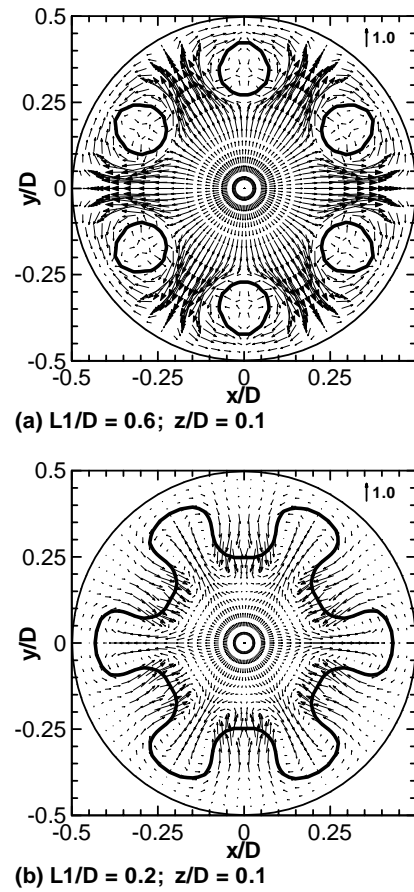


Fig. 13 Velocity vectors for the cases shown in Fig. 12(b) and d. The sections are taken at  $z/D = 0.1$ . The solid line represents the mixture fraction surface ( $\xi = 0.055$  and  $Re_D = 200$ ).

In Fig. 13 (a), the solid lines corresponding to the mixture fraction surface  $\xi = 0.055$  show very clearly the locations of the oxidizer jets. In Fig. 13 (a) there is a strong flow of the fuel stream into the region between the jets. This is evidenced by the large arrows in the positive radial direction in these regions. For the case shown in Fig. 13 (b) where the overall mixing performance is much poorer (cf. Fig. 12 (d)), the flow of the fuel stream into the regions between the jets is greatly reduced and the fuel-rich region (given by  $\xi > 0.055$ ) does not encircle the oxidizer jets. A close examination of the velocity vectors in the center of the oxidizer jets, for example at  $x/D = 0$  and  $y/D = 0.35$  in Fig. 13, shows that there is a considerably greater negative radial component of velocity at this location for Fig. 13 (b) than for Fig. 13 (a). It is not unreasonable to suppose that for the case of Fig. 13 (b) the oxidizer jets have been deflected towards the center of the chamber due to the positioning of the backward facing step on the upstream side of the baffle plate shown in Fig. 12 (d). Thus the jet angle has

been altered and a rather different flow and mixing pattern inside the chamber has resulted.

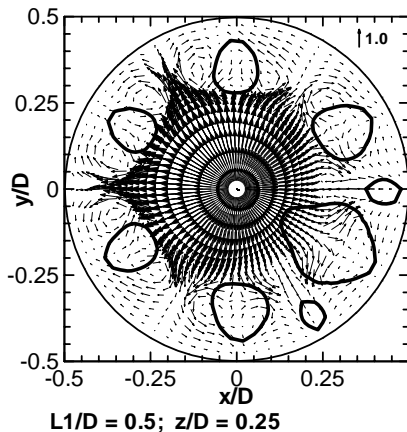


Fig. 14 Velocity vectors for the non-symmetric case in Fig. 12. The cross section is taken at  $z/D = 0.25$ . The solid line represents the mixture fraction iso-surface,  $\xi = 0.055$ ,  $Re = 200$ .

Moving on to the non-symmetrical case shown in Fig. 12 (c), it should be noted that the final level of convergence for this case was quite good suggesting that it is in fact a valid solution to the governing equations. Figure 14 shows a z-cross section for this case at a position  $z/D = 0.25$ . The results indicate some degree of symmetry, but not the full symmetry for the cases shown in Fig. 13.

While somewhat undesirable from an engineering design point of view, the non-symmetrical result is fascinating from the perspective of fluid dynamics. It demonstrates that for perfectly symmetrical geometry and boundary conditions a non-symmetrical solution can arise. In this case the fuel jet, instead of being divided evenly among the surrounding oxidizer jets, has taken a special 'liking' to one jet in the top left-hand corner of Fig. 14. This kind of non-symmetrical phenomenon, although well known for cases such as the double-sided backward facing step perhaps has not been reported as widely for multiple confined jet arrays. Thus, in modeling this kind of combustor it is better to follow the present procedure to include the whole domain in the calculation rather than employ symmetry boundaries where the geometry is symmetrical.

In concluding this section on the case with  $Re_D = 200$ , it is clear that for laminar flow, as Reynolds number is increased so also is the need for consideration of the effects of upstream flow conditions prior to the combustion chamber.

## CONCLUSIONS

In summing up this investigation on the effects of upstream conditions a number of conclusions can be drawn as follows:

1. Using an unstructured finite-volume technique the proposed combustor design was simulated and shown to perform well in terms of flow mixing over a range of upstream inlet conditions for laminar flow.

2. For practical calculation it is better to start the computational domain on the upstream side of the baffle plate rather than directly at the inlet to the chamber.
3. The present baffle plate design was generally shown to have a smoothing effect on the upstream conditions thus reducing the influence on the mixing pattern in the chamber.
4. If introduced one diameter upstream of the baffle plate, a large component of swirl is necessary in order to have a noticeable effect on the mixing pattern inside the chamber.
5. For a Reynolds number of 100 while some degree of asymmetry may be permissible in the flow at a distance of one can diameter upstream of the baffle plate, it is highly desirable that the upstream inlet conditions be symmetrical to increase the likelihood of a symmetrical mixing pattern inside the chamber.
6. For at least one set of flow conditions it was found that a non-symmetrical flow pattern could result inside the chamber in spite of the fact that the geometry and boundary conditions were symmetrical. Thus it is better to include the full domain in a computation rather than assume symmetry boundaries at locations where the geometry is symmetrical.
7. Finally, for laminar flow, the higher the Reynolds number the more care is likely to be required in preparing the inlet conditions for a practical combustor.

## ACKNOWLEDGMENTS

This work was supported through the project "Micro Gas Turbine / Fuel Cell Hybrid-Type Distributed Energy System" by the Japan Science and Technology Corporation (JST) as Core Research of Evolutional Science and Technology (CREST). The support of the Japan Society for the Promotion of Science (JSPS) for the first author is gratefully acknowledged

## REFERENCES

1. Suzuki, K., Kim, J. H. and Teshima, K., 2000, "Solid oxide fuel cell and micro gas turbine hybrid cycle for a distributed energy generation system", Key-note, Proceedings, 4<sup>th</sup> KSME-JSME Thermal Engineering Conference, Kobe, Japan, pp. 1 - 7.
2. Woodfield, P. L., Nakabe, K. and Suzuki, K., 2003, "Numerical study for enhancement of laminar flow mixing using multiple confined jets in a micro can combustor", International Journal of Heat and Mass Transfer, (in press).
3. Woodfield, P. L., Nakabe, K. and Suzuki, K., 2003, "Performance of a three-dimensional pressure-based unstructured finite-volume method for low Reynolds number flow and wall heat transfer rate prediction", Numerical Heat Transfer, B (in press).
4. Rhie, C. M. and Chow, W. L., 1983, "Numerical study of the turbulent flow past an airfoil with trailing edge separation", AIAA Journal, **21**, pp. 1525 - 1532.
5. Jiang, B., Lin, T. L. and Povinelli, L. A., 1994, "Large-scale computation of incompressible viscous flow by least-squares finite element method", Comput. Methods Appl. Mech. Engrg. **114**, pp. 213 - 231.